Journal of Imaging Science and Technology® 66(6): 060405-1–060405-10, 2022.

Estimation of Motion Sickness in Automated Vehicles using Stereoscopic Visual Simulation

Yoshihiro Banchi▲ and Takashi Kawai

Department of Intermedia Art and Science, School of Fundamental Science and Engineering, Waseda University, 3-4-1 Okubo, Shinjuku, Tokyo 169-8555, Japan

E-mail: y.banchi@aoni.waseda.jp

Abstract. *Automation of driving leads to decrease in driver agency, and there are concerns about motion sickness in automated vehicles. The automated driving agencies are closely related to virtual reality technology, which has been confirmed in relation to simulator sickness. Such motion sickness has a similar mechanism as sensory conflict. In this study, we investigated the use of deep learning for predicting motion. We conducted experiments using an actual vehicle and a stereoscopic image simulation. For each experiment, we predicted the occurrences of motion sickness by comparing the data from the stereoscopic simulation to an experiment with actual vehicles. Based on the results of the motion sickness prediction, we were able to extend the data on a stereoscopic simulation in improving the accuracy of predicting motion sickness in an actual vehicle. Through the performance of stereoscopic visual simulation, it is considered possible to utilize the data in deep learning.* © *2022 Society for Imaging Science and Technology.*
[DOI: 10.2352/J.ImagingSci.Technol.2022.66.6.060405]

1. INTRODUCTION

Autonomous driving technology is making great progress through advanced sensing technology such as LIDAR and advanced computing technology such as image analysis using deep learning. Although fully automated driving has yet to be achieved, driver assistance systems have made it possible for drivers to drive without having to operate most driving aspects in recent years. Automated driving can be categorized into levels according to the degree of automation [1, 2]. As various countries continue to establish laws and regulations related to automated driving, vehicles with level 3 performance have started to appear in the market. As the level of automated driving progresses, the necessity for drivers to operate the vehicle decreases, and at level 5, the driver does not need to operate the vehicle at all.

One aspect of concern with driver engagement becoming completely unnecessary is automated driving motion sickness. One of the reasons why drivers do not tend to get motion sickness is the effect of agency on such motion sickness. We learned, for example, that susceptibility to inducing motion sickness differs according to the type of agency, and, in automobiles, passengers (those sitting in the passenger seat) are more likely to be affected than drivers [3]. Particularly, motion sickness can occur due to the decrease in driver agency caused by automated driving. Hence, there are chances that automated driving motion sickness may occur [4]. As it is necessary for the driver to operate the vehicle, up to level 5, in case of emergencies, paying attention to the driver's condition in addition to controlling the vehicle is necessary.

Agency is also thought to play a part in simulator-based motion sickness. Agency is related to presence [5], and we know that this affects simulator-based motion sickness [6]. On the other hand, in technologies such as virtual reality (VR), agency and immersion are positioned as important elements; therefore, there are concerns about the occurrence of simulator-based motion sickness and VR-based motion sickness [7, 8].

One cause of motion sickness, including automated driving motion sickness and simulator-based motion sickness, is the sensory conflict [9]. The sensory conflict theory states that motion sickness is caused by visual or somatosensory information that is inconsistent with expected information based on past experience. Automated driving can also be viewed as a type of sensory conflict, and the degree of conflict is thought to increase further when the driver engages in activities other than driving the vehicle. One difference between automated driving motion sickness and simulator-based motion sickness is that in simulator-based motion sickness, sensory information is presented, whereas, in automated driving motion sickness, somatosensory information is not presented. Therefore, studies have been conducted on mitigation techniques, such as matching visual and somatosensory information [10] and limiting visual information [11] to reduce motion sickness. Furthermore, in terms of in-vehicle behavior linked to automated driving, VR-based experiments have also been conducted to link the presentation of somatosensory information with visual information [12].

Studies are being conducted to evaluate motion sickness and predict the occurrence of the same. To use objective indicators to evaluate motion sickness, many correlations between objective indicators and motion sickness have been investigated [13–15]. In recent years, such investigations have used machine learning [16–18]. Although these studies were able to assess heart rate (HR), electromyography (EMG), and electroencephalography (EEG), it is difficult to

▲ IS&T Member.

Received July 1, 2022; accepted for publication Nov. 10, 2022; published online Dec. 1, 2022. Associate Editor: Danli Wang.

1062-3701/2022/66(6)/060405/10/$25.00

attach a sensor to other indicators, thereby making it unrealistic to implement machine learning. By using machine learning however, it is possible to evaluate relationships based on multiple and single objective indicators. When examining human behavior, machine learning is able to predict a fixed level of accuracy [19, 20], and if this is possible in the area of motion sickness, it could contribute to resolving issues related to the onsets of motion sickness.

Researchers have attempted to estimate the occurrence of cybersickness, which is a type of motion sickness [21]. In the mixed reality (MR) environment, we obtained different indicators concerning discomfort and general physiology while puzzle assembly tasks were continuously performed. Then, we estimated the discomfort based on the physiological indicators using a deep learning model. The results suggested that it was possible to predict the onset of cybersickness to a certain extent. However, it is said that a high number of samples is generally required for machine learning, and it is difficult to secure a high number of samples based on a test environment.

2. PURPOSE

In this study, we aimed to develop a system than predicts the occurrence and early detection of motion sickness for automated driving. However, due to the COVID crisis, and based on similarities in mechanisms such as sensory conflict, this study also aims to examine data expansion using stereoscopic simulation.

3. METHODS

3.1 *Driving an Actual Vehicle (Experiment 1)*

3.1.1 *Measures*

As a subjective indicator, participants were asked to respond every 10 s in regard to three levels of motion sickness (1: No sickness, 2: Slight sickness, or 3: High sickness). In the prediction of motion sickness in automobiles, it is considered essential to predict it early and encourage rest, especially regarding the motion sickness of the driver. For this reason, we placed particular importance on detecting the slight motion sickness stage or no sickness, so data acquisition was set to three levels. As objective indicators, HOT-2000 (NeU) was used to acquire cerebral blood flow, pulse rate, and acceleration, while electrodermal activity (EDA) was acquired using biosignalsplux (10 Hz). Low-frequency (LF) and high-frequency (HF) bands were also calculated based on the pulse rate.

3.1.2 *Stimuli*

For the driving course, several driving patterns were set in advance, and from these, several patterns wherein motion sickness could easily occur were selected. The course consisted of a combination of left and right turns and emergency braking/emergency acceleration. The content of the driving course is summarized in Table I. All the drivers were trained to drive at the same pace.

Table I. Driving course.

Time (sec)	Driving patterns
0–15	Sharp cutbacks left and right
15–35	Turning 2.5 times to the left
35–55	Turning 2.5 times to the right
55–65	Stop by emergency brake/emergency acceleration × 3 times
65–95	Turn three times in a Figure 8 pattern
95–105	Sharp cutbacks left and right
105–125	Turning three times to the left
125–130	Stopping using the emergency brake

3.1.3 *Procedure*

Eleven adult drivers participated in the experiment. The purpose of the experiment and what the participants had to do in the experiment was explained and informed consent was obtained from them. Participant was explained that 1 (Slight sickness) is a different state from 0 (No sickness), and evaluation as 1 should be made when feeling even a little sick. Then, various devices were attached for measurement purposes, and the participants were asked to sit in the passenger seat. To ensure stable measurement and posture, they placed their left hands on a jig and lightly gripped the door handle with their right hand as if holding it. The discomfort level was checked before starting the experiment, and the participants only had to verbally rate their discomfort level every 10 s during the experiment. The sound to be evaluated was confirmed and the experiment was started. From the start of the drive, participants verbally rated their discomfort according to a cue from an electronic metronome every 10 s. When a participant suffered extreme motion sickness, the experiment was stopped.

3.2 *Simulation through Stereoscopic Imaging (Experiment 2)*

3.2.1 *Measures*

The indicators of Experiment 1 were acquired for the simulation experiment. Specifically, as a subjective indicator, participants were asked to respond every 10 s in regard to three levels of motion sickness: (1: Nothing, 2: Slightly Sickness, or 3: Highly Sickness). As objective indicators, cerebral blood flow, pulse rate, acceleration, and EDA were obtained (10 Hz). LF and HF bands were also calculated based on the pulse rate.

3.2.2 *Stimuli*

VR cameras were attached to the participants' heads, and the course run in Experiment 1 was captured (Figure 1). An Insta360EVO capable of capturing 3DVR180 videos was used as the VR camera. The video size was 3840 × 3840 px (one eye: 3840 × 1920, 50 fps, 20 Mbpm) and the duration was 130 s.

Figure 1. VR camera attached to the participant's head.

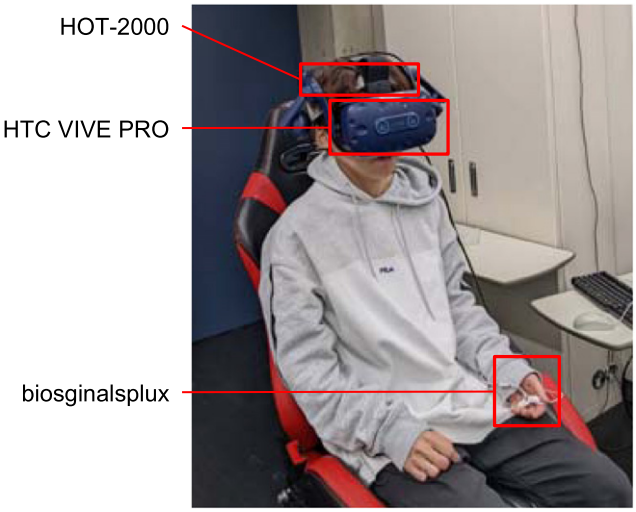

Figure 2. Layout of the stereoscopic visual simulation experiment.

3.2.3 *Procedure*

A total of 54 adults participated in the experiment. The purpose of the experiment and what the participants had to do in the experiment was explained and informed consent was obtained from them. Participant was explained that 1 (Slight sickness) is a different state from 0 (No sickness), and evaluation as 1 should be made when feeling even a little sick. Then, various measurement devices were attached, and participants were asked to sit in the bucket seat to begin the simulation (Figure 2). VIVE Pro VR headset (HTC) was used for presenting the VR video stimuli. The discomfort level was checked before starting the experiment, and the participants only had to verbally rate their discomfort level every 10 s during the experiment. From the start of the video, participants verbally rated their discomfort based on an electronic metronome cue every 10 s.

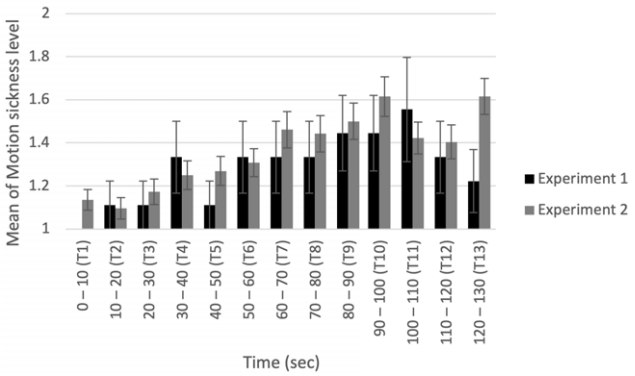

Figure 3. Transition of motion sickness.

4. RESULTS

Within each indicator, there were many participant data and time interval data with missing values, and these were excluded from the analysis data. For this reason, the result was analyzed for only 9 people in Experiment 1 and 52 in Experiment 2.

4.1 *Subjective Indicators*

(1) Real vehicle experiment (Experiment 1)

In regard to the three levels of motion sickness, there were 85 cases of 1 (No sickness), 31 cases of 2 (Slight Sickness), and 1 case of 3 (High Sickness). The transition of motion sickness for each time interval is shown in Figure 3 on Experiment 1. In the plots, the horizontal axis indicates the time interval, and the vertical axis indicates the average of motion sickness in all participants. Significant differences were seen in one-way repeated measures ANOVA with time interval ($F(12, 96) = 2.216$, $p = 0.017$, and $\eta^2 = 0.109$). Shaffer post-hoc paired test with time factor was conducted but there were no significant differences.

(2) Stereoscopic visual simulation

In regard to the three levels of motion sickness, there were 456 cases of 1 (No sickness), 196 cases of 2 (Slight Sickness), and 24 cases of 3 (High Sickness). The transition for each time interval is shown in Fig. 3 on Experiment 2. In the plots, the horizontal axis indicates the time interval, and the vertical axis indicates the average of motion sickness in all participants. Significant differences were seen in one-way repeated measures ANOVA with time interval ($F(12, 612) = 11.736$, $p < 0.001$, and $\eta^2 = 0.090$). Shaffer post-hoc paired test with time factor showed significant differences in Time 0-10 sec (T1)–T9, T10, T13, T2–T7, T8, T9, T10, T11, T12, T13, T3–T7, T8, T9, T10, T13, T4–T9, T10, T13, T5–T10, T13, T6–T10, and T13 (Table A1 and Table A2).

4.2 *Objective Indicators*

To judge the correspondence with the subjective indicators, we calculated the mean value of each indicator, using 10 s as an interval. Additionally, the objective indicators used were EDA, pulse rate, and LF/HF, and each participant was normalized from −1 by MinMaxScaler to see the variation.

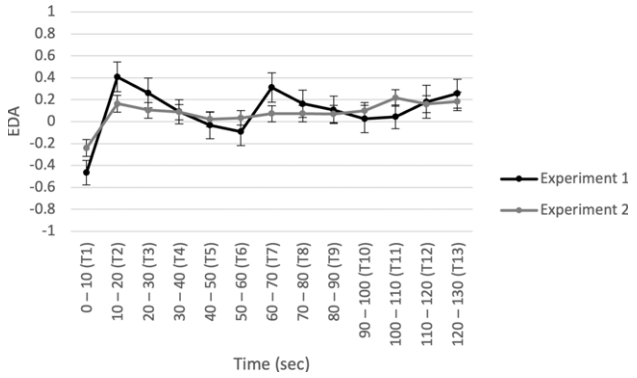

Figure 4. Results of EDA.

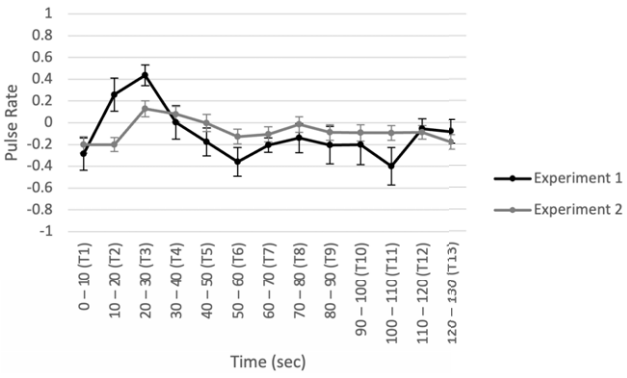

Figure 5. Results of Pulse Rate.

4.2.1 *EDA*

(1) Real vehicle experiment (Experiment 1)

The mean values and standard error for each time interval are shown in Figure 4 on Experiment 1. The mean value before normalization was 9.16 (μS). Significant differences were seen in one-way repeated measures ANOVA with time interval ($F(12, 96) = 4.142, p < 0.001, \eta^2 = 0.259$). Shaffer post-hoc paired test with time factor showed a significant difference between T1 and T2.

(2) Stereoscopic visual simulation

The mean values and standard error for each time interval are shown in Fig. 4 on Experiment 2. The mean value before normalization was 8.14 (μS). Significant differences were seen in one-way repeated measures ANOVA with time interval ($F(12, 96) = 3.604, p < .001$, and $\eta^2 = 0.039$). Shaffer post-hoc paired test with time factor showed significant differences between T1–T2, T3, T4, and T11 (Table A3 and Table A4).

4.2.2 *Pulse Rate*

(1) Real vehicle experiment (Experiment 1)

The mean values and standard error for each time interval are shown in Figure 5 on Experiment 1. The mean value before normalization was 101.47 (bpm). Significant differences were seen in one-way repeated measures ANOVA with time interval ($F(12, 96) = 3.969, p < 0.001$, and $\eta^2 = 0.250$). Shaffer post-hoc paired test with time factor showed significant differences between T3 and T7.

(2) Stereoscopic visual simulation

The mean values and standard error for each time interval are shown in Fig. 5 on Experiment 2. The mean value before normalization was 83.71 (bpm). Significant differences were seen in one-way repeated measures ANOVA with time interval ($F(12, 96) = 4.311, p < 0.001$, and $\eta^2 = 0.036$). Shaffer post-hoc paired test with time factor showed significant differences between T1–T3, T2–T3, T4, T3–T6, and T4–T6 (Table A5 and Table A6).

4.2.3 *LF/HF*

(1) Real vehicle experiment (Experiment 1)

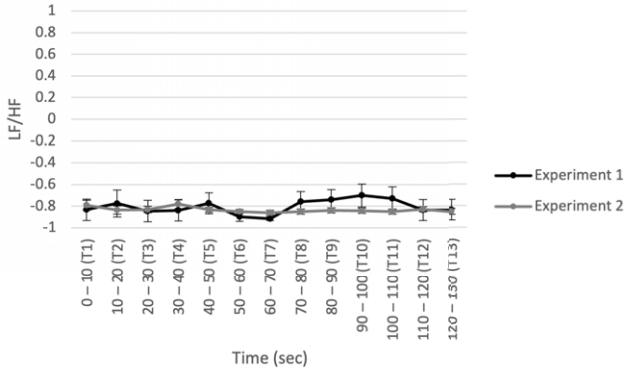

Figure 6. Result of LF/HF.

The mean values and standard error for each time interval are shown in Figure 6 on Experiment 1. The mean value before normalization was 2.85. Significant differences were not seen in one-way repeated measures ANOVA with time interval ($F(12, 96) = 1.595, p = 0.106$, and $\eta^2 = 0.052$).

(2) Stereoscopic visual simulation

The mean values and standard error for each time interval are shown in Fig. 6 on Experiment 2. The mean value before normalization was 3.06. Significant differences were not seen in one-way repeated measures ANOVA with time interval ($F(12, 96) = 1.258, p = 0.240$, and $\eta^2 = 0.011$).

5. PREDICTION OF MOTION SICKNESS USING DEEP LEARNING

5.1 *Model*

For the model to predict motion sickness, a deep learning model based on one-dimensional convolutional neural network (1DCNN) was used. The prediction was performed using a recurrent neural network (RNN); however, as the 1DCNN model had higher precision, we reported the 1DCNN model results. The model had three layers–convolution, pooling, and dropout–and two fully connected layers. In the first fully connected layer, we input the predicted value for motion sickness in the previous interval. Leaky ReLU was used as the activation function, and Softmax

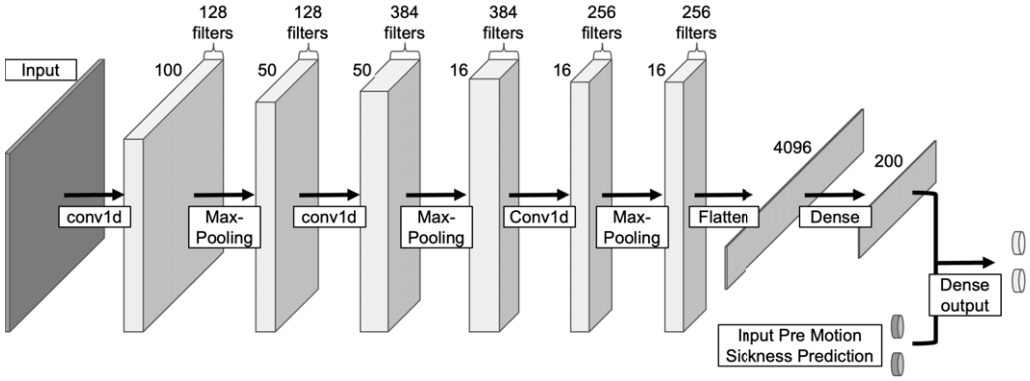

Figure 7. Image of the model used for predicting motion sickness.

Table II. Confusion matrix of Experiment 1.

		MS level		PREDICTION 0: Nothing	PREDICTION 1: Sickness
Cross validation	1	TRUE	0	17	0
			1	4	11
	2		0	20	5
			1	2	5
	3		0	25	1
			1	1	4
	4		0	19	3
			1	5	4

Table III. Confusion matrix of Experiment 2.

		MS level		PREDICTION 0: Nothing	PREDICTION 1: Sickness
Cross validation	1	TRUE	0	103	18
			1	8	43
	2		0	93	17
			1	10	51
	3		0	104	9
			1	10	48
	4		0	111	5
			1	30	25

was used as the output layer. The categorical cross-entropy loss function and Adam optimization algorithm were used. An image of the model is shown in Figure 7.

5.2 *Datasets*

Data with missing values were excluded, so datasets were for 9 people in Experiment 1 and 52 in Experiment 2 and the data were divided every 10 s to predict motion sickness levels. For objective indicators, EDA, pulse rate, and LF/HF were used. Each indicator was normalized in the MinMaxScaler as −1–1 for each participant. When predicting motion sickness, as there were few cases of 3 (High Sickness), it was considered to be 0 (No sickness) as 1 (No Sickness), and 1 (Sickness) as 2 (Slight Sickness) and 3 (High Sickness). So that the data of Experiment 1 is based on 85 cases of 0, 32 cases of 1, and the data of Experiment 2 is based on 456 cases of 0, 220 cases of 1.

5.3 *Real Vehicle Experiment (Experiment 1)*

For accuracy verification, the average value of the results in four-fold cross-validation randomly in person and time was used. A summary of the confusion matrix of the four sessions is shown in Table II. The mean accuracy of the four sessions was 0.833, with the F1-score for "Nothing" being 0.883 and F1-score for "Sickness" being 0.684.

5.4 *Stereoscopic Visual Simulation*

For accuracy verification, the average value of the results in the four-fold cross-validation randomly in person and time was used. A summary of the confusion matrix of the four sessions is shown in Table III. The mean accuracy for the four sessions was 0.844, with the F1-score for "Nothing" being 0.885 and F1-score for "Sickness" being 0.745.

5.5 *Stereoscopic Visual Simulation and Real Vehicle Experiments (Experiment 1 and 2)*

To validate the effect of expanding the training data from Experiment 2, a four-fold cross-validation was performed on Experiment 1 data. The data from the stereoscopic video experiment was also added to the training data (Figure 8). A summary of the confusion matrix for the four sessions is shown in Table IV. The mean accuracy for the four sessions was 0.866, with the F1-score for "Nothing" being 0.896 and F1-score for "Sickness" being 0.754.

6. DISCUSSION

6.1 *Subjective Indicators*

It is known that the user experience changes with viewing time in VR [22]. Thus, the effect of time and somatosensory information was analyzed by comparing Experiment 1 and Experiment 2. The results of the actual vehicle experiment

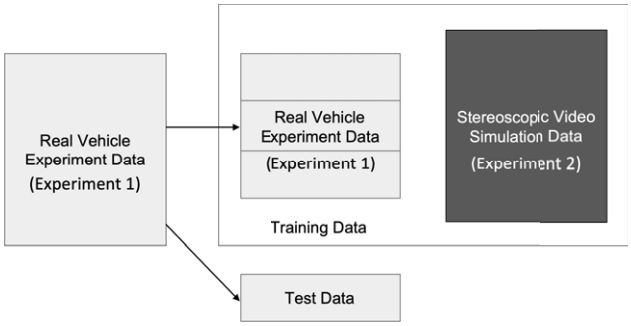

Figure 8. Image of stereoscopic visual simulation's extended learning datasets.

Table IV. Stereoscopic visual simulation extension confusion matrix.

		MS level		PREDICTION 0: Nothing	PREDICTION 1: Sickness
Cross validation	1	TRUE	0	13	4
			1	1	14
	2		0	20	5
			1	1	6
	3		0	24	2
			1	2	3
	4		0	20	2
			1	0	9

demonstrated a tendency for motion sickness to increase, with a peak at the 110-s interval. The results of the stereoscopic visual experiment demonstrated a tendency for motion sickness to increase, with a peak at the 100- and 130-s intervals. Where each experiment demonstrated an increasing trend, the fact that the position of the peak differs is thought to be due to the fact that the degree of sensory conflict differs in the various cases of vehicle sickness and simulation sickness. Particularly, it is affected by the presence or absence of somatosensory information being presented.

6.2 *Objective Indicators*

Compared to the real vehicle experiment, each indicator in the stereoscopic visual experiment tended to vary by only a small degree. In the results of ANOVA for the real vehicle experiment, a large effect size was seen for EDA and HR, whereas a small effect size was seen for LF/HF bands. Furthermore, in the results of ANOVA for the stereoscopic visual experiment, a small degree of change was seen for all participants. This suggests that the response of the objective index was greater for the real vehicle than for the stereoscopic visuals.

If we compare the peak positions for the objective and subjective indicators, we can see that the peak position does not match for any participants. This suggests that evaluating the response to specific objective indicators and subjective indicators is difficult.

6.3 *Predicting Motion Sickness*

The cross-validation accuracy of the real vehicle test was 0.833, and the cross-validation accuracy of the stereoscopic visual experiment was 0.844. When the learning data used in the stereoscopic visual experiment was extended, the cross-validation accuracy was 0.866. In a previous study, predicting the motion sickness levels through a self-organizing neural fuzzy inference network (SONFIN) using EEG signals, an overall accuracy of about 82% through experiments was achieved [23]. When predicting motion sickness levels through a three-dimensional convolutional neural network (3DCNN) using 3D image information, the correlation between a simulator sickness questionnaire (SSQ) [24] and prediction score was 0.845 [25]. When predicting the VR sickness levels through a Deep Long Short Term Memory Model (LSTM) using posture instability signal, the correlation between a SSQ and prediction score was 0.89 [26]. These results suggest that the accuracy for predicting motion sickness within the respective tests could be predicted with constant accuracy. Therefore, it is thought that the objective indicators obtained in this study can contribute to predicting motion sickness to some extent. Additionally, by adding the stereoscopic visual simulation data to the real vehicle experiment, it was confirmed that the accuracy for predicting motion sickness in the real vehicle experiment could be improved. Thus, even when data is obtained under different environments, the data capture common responses within the scope of sensory conflict.

7. SUMMARY

In this study, we attempted to predict motion sickness in automated driving based on data extensions through a stereoscopic visual simulation. We conducted a real vehicle experiment and a stereoscopic visual simulation and predicted the presence or absence of motion sickness using deep learning. We confirmed that it was possible to predict motion sickness in a real vehicle with a consistent level of accuracy. Moreover, we were able to extend the learning data using stereoscopic visual simulation, and it was suggested that this may improve accuracy in predicting motion sickness in actual vehicles. This suggests that in environments where it is difficult to conduct experiments with real objects, data acquisition through stereoscopic image simulations can be utilized for deep learning and other data applications. Moreover, as different tendencies were observed in individual indicators, such as objective and subjective indicators, it is necessary to be careful when handling the data.

ACKNOWLEDGMENT

The authors would like to thank Mahiro Ito, Yusuke Ohira, Shintaro Kakuda, Haruka Kato, Taisei Tsukahara, Soichiro Sawai and Yuki Takagi for support with the experiments. This work is supported by the AISIN CORPORATION.

APPENDIX

Table A1. Post-hoc test results of Subjective indicators of Real vehicle experiment (Experiment 1).

		p-value												
		0–10 sec T1	10–20 T2	20–30 T3	30–40 T4	40–50 T5	50–60 T6	60–70 T7	70–80 T8	80–90 T9	90–100 T10	100–110 T11	110–120 T12	120–130 T13
t-value	T1	–	0.347	0.347	0.081	0.347	0.081	0.081	0.081	0.035	0.035	0.051	0.081	0.169
	T2	1.000	–	1.000	0.169	1.000	0.169	0.169	0.169	0.081	0.081	0.104	0.169	0.347
	T3	1.000	0.000	–	0.169	1.000	0.169	0.169	0.169	0.081	0.081	0.104	0.169	0.347
	T4	2.000	1.512	1.512	–	0.169	1.000	1.000	1.000	0.347	0.347	0.169	1.000	0.347
	T5	1.000	0.000	0.000	1.512	–	0.169	0.169	0.169	0.081	0.081	0.104	0.169	0.347
	T6	2.000	1.512	1.512	0.000	1.512	–	1.000	1.000	0.594	0.347	0.169	1.000	0.347
	T7	2.000	1.512	1.512	0.000	1.512	0.000	–	1.000	0.347	0.594	0.347	1.000	0.347
	T8	2.000	1.512	1.512	0.000	1.512	0.000	0.000	–	0.347	0.594	0.347	1.000	0.347
	T9	2.530	2.000	2.000	1.000	2.000	0.555	1.000	1.000	–	1.000	0.594	0.347	0.169
	T10	2.530	2.000	2.000	1.000	2.000	1.000	0.555	0.555	0.000	–	0.347	0.347	0.169
	T11	2.294	1.835	1.835	1.512	1.835	1.512	1.000	1.000	0.555	1.000	–	0.169	0.081
	T12	2.000	1.512	1.512	0.000	1.512	0.000	0.000	0.000	1.000	1.000	1.512	–	0.347
	T13	1.512	1.000	1.000	1.000	1.000	1.000	1.000	1.000	1.512	1.512	2.000	1.000	–

Table A2. Post-hoc test results of Subjective indicators of Stereoscopic visual experiment (Experiment 2).

		p-value												
		0–10 sec T1	10–20 T2	20–30 T3	30–40 T4	40–50 T5	50–60 T6	60–70 T7	70–80 T8	80–90 T9	90–100 T10	100–110 T11	110–120 T12	120–130 T13
t-value	T1	–	0.485	0.569	0.057	0.051	0.019	0.001	0.001	0.000	0.000	0.001	0.002	0.000
	T2	0.704	–	0.044	0.004	0.002	0.002	0.000	0.000	0.000	0.000	0.000	0.000	0.000
	T3	0.574	2.062	–	0.103	0.058	0.051	0.000	0.000	0.000	0.000	0.001	0.002	0.000
	T4	1.948	3.045	1.660	–	0.569	0.371	0.006	0.006	0.000	0.000	0.028	0.019	0.000
	T5	1.996	3.267	1.939	0.574	–	0.569	0.006	0.011	0.002	0.000	0.044	0.018	0.000
	T6	2.431	3.335	1.996	0.903	0.574	–	0.019	0.070	0.017	0.000	0.159	0.255	0.000
	T7	3.477	5.419	4.173	2.844	2.850	2.414	–	0.742	0.532	0.031	0.622	0.444	0.059
	T8	3.451	5.196	3.965	2.850	2.635	1.849	0.331	–	0.261	0.019	0.785	0.532	0.019
	T9	4.428	5.878	4.592	3.756	3.267	2.470	0.629	1.137	–	0.083	0.322	0.168	0.135
	T10	5.405	5.838	5.250	4.428	4.229	4.382	2.217	2.431	1.767	–	0.017	0.015	1.000
	T11	3.438	4.592	3.472	2.268	2.062	1.428	0.496	0.275	1.000	2.470	–	0.709	0.006
	T12	3.247	4.761	3.267	2.414	2.442	1.151	0.772	0.629	1.400	2.521	0.375	–	0.002
	T13	5.683	6.908	5.915	4.696	4.804	4.081	1.935	2.431	1.519	0.000	2.850	3.335	–

Table A3. Post-hoc test results of EDA of Real vehicle experiment (Experiment 1).

		p-value												
		0-10 sec	10–20	20–30	30–40	40–50	50–60	60–70	70–80	80–90	90–100	100–110	110–120	120–130
		T1	T2	T3	T4	T5	T6	T7	T8	T9	T10	T11	T12	T13
t-value	T1	–	0.000	0.002	0.006	0.048	0.071	0.006	0.017	0.028	0.044	0.029	0.025	0.009
	T2	5.829	–	0.155	0.042	0.046	0.044	0.609	0.278	0.201	0.126	0.133	0.371	0.514
	T3	4.431	1.569	–	0.027	0.049	0.055	0.753	0.591	0.447	0.267	0.301	0.727	0.975
	T4	3.662	2.414	2.710	–	0.109	0.109	0.146	0.634	0.919	0.684	0.764	0.640	0.381
	T5	2.336	2.364	2.314	1.806	–	0.368	0.038	0.172	0.330	0.673	0.539	0.219	0.122
	T6	2.078	2.393	2.241	1.803	0.954	–	0.027	0.071	0.179	0.370	0.241	0.091	0.069
	T7	3.700	0.533	0.325	1.609	2.481	2.692	–	0.057	0.037	0.029	0.086	0.405	0.682
	T8	2.993	1.164	0.559	0.495	1.499	2.086	2.227	–	0.376	0.088	0.262	0.860	0.404
	T9	2.682	1.392	0.800	0.105	1.037	1.474	2.498	0.938	–	0.057	0.398	0.437	0.082
	T10	2.391	1.708	1.193	0.422	0.437	0.951	2.663	1.946	2.221	–	0.666	0.079	0.005
	T11	2.646	1.672	1.105	0.310	0.642	1.266	1.960	1.208	0.893	0.448	–	0.108	0.025
	T12	2.759	0.948	0.362	0.486	1.335	1.922	0.878	0.182	0.819	2.012	1.811	–	0.457
	T13	3.425	0.683	0.032	0.926	1.727	2.097	0.425	0.881	1.991	3.809	2.764	0.782	–

Table A4. Post-hoc test results of EDA of Stereoscopic visual experiment (Experiment 2).

		p-value												
		0–10 secc	10–20	20–30	30–40	40–50	50–60	60–70	70–80	80–90	90–100	100–110	110–120	120–130
		T1	T2	T3	T4	T5	T6	T7	T8	T9	T10	T11	T12	T13
t-value	T1	–	0.000	0.000	0.000	0.005	0.006	0.007	0.007	0.011	0.006	0.000	0.002	0.003
	T2	6.517	–	0.135	0.222	0.068	0.142	0.358	0.400	0.423	0.589	0.658	0.978	0.875
	T3	4.792	1.519	–	0.668	0.154	0.313	0.697	0.735	0.739	0.961	0.310	0.636	0.538
	T4	4.250	1.238	0.432	–	0.039	0.312	0.838	0.859	0.844	0.895	0.183	0.482	0.403
	T5	2.972	1.867	1.447	2.123	–	0.705	0.347	0.349	0.443	0.305	0.025	0.136	0.122
	T6	2.849	1.495	1.019	1.021	0.380	–	0.303	0.420	0.519	0.348	0.022	0.148	0.141
	T7	2.834	0.928	0.392	0.205	0.951	1.041	–	0.974	0.971	0.639	0.040	0.263	0.246
	T8	2.811	0.850	0.341	0.178	0.947	0.813	0.033	–	0.907	0.533	0.026	0.221	0.213
	T9	2.637	0.809	0.335	0.197	0.774	0.649	0.037	0.118	–	0.338	0.010	0.166	0.176
	T10	2.861	0.545	0.050	0.133	1.036	0.948	0.472	0.628	0.967	–	0.015	0.268	0.237
	T11	3.808	0.446	1.027	1.353	2.316	2.375	2.111	2.293	2.688	2.528	–	0.028	0.592
	T12	3.252	0.028	0.477	0.708	1.517	1.471	1.133	1.240	1.407	1.120	2.270	–	0.545
	T13	3.198	0.159	0.620	0.844	1.576	1.498	1.175	1.263	1.373	1.197	0.539	0.609	–

Table A5. Post-hoc test results of Pulse rate of Real vehicle experiment (Experiment 1).

		p-value												
		0–10 sec	10–20	20–30	30–40	40–50	50–60	60–70	70–80	80–90	90–100	100–110	110–120	120–130
		T1	T2	T3	T4	T5	T6	T7	T8	T9	T10	T11	T12	T13
t-value	T1	–	0.033	0.006	0.085	0.542	0.672	0.560	0.479	0.726	0.709	0.588	0.291	0.322
	T2	2.569	–	0.374	0.379	0.134	0.046	0.013	0.151	0.126	0.146	0.041	0.154	0.152
	T3	3.665	0.941	–	0.038	0.003	0.001	0.000	0.003	0.009	0.021	0.006	0.006	0.003
	T4	1.966	0.932	2.488	–	0.047	0.001	0.155	0.308	0.272	0.275	0.041	0.778	0.534
	T5	0.636	1.668	4.201	2.347	–	0.005	0.819	0.600	0.792	0.830	0.105	0.466	0.360
	T6	0.439	2.366	4.755	4.790	3.843	–	0.263	0.054	0.257	0.217	0.753	0.095	0.045
	T7	0.608	3.208	5.848	1.568	0.237	1.205	–	0.642	0.998	0.986	0.299	0.312	0.322
	T8	0.743	1.588	4.117	1.088	0.547	2.255	0.483	–	0.410	0.571	0.070	0.532	0.581
	T9	0.363	1.711	3.404	1.181	0.273	1.221	0.003	0.870	–	0.949	0.092	0.387	0.352
	T10	0.387	1.609	2.865	1.172	0.222	1.340	0.018	0.590	0.066	–	0.013	0.439	0.447
	T11	0.564	2.433	3.712	2.435	1.830	0.326	1.111	2.088	1.912	3.179	–	0.104	0.068
	T12	1.130	1.575	3.711	0.292	0.765	1.892	1.079	0.654	0.916	0.814	1.836	–	0.852
	T13	1.055	1.584	4.173	0.650	0.971	2.381	1.055	0.575	0.989	0.800	2.111	0.193	–

Table A6. Post-hoc test results of Pulse rate of Stereoscopic visual experiment (Experiment 2).

		p-value												
		0–10 sec	10–20	20–30	30–40	40–50	50–60	60–70	70–80	80–90	90–100	100–110	110–120	120–130
		T1	T2	T3	T4	T5	T6	T7	T8	T9	T10	T11	T12	T13
t-value	T1	–	0.965	0.000	0.002	0.052	0.368	0.273	0.026	0.212	0.216	0.223	0.209	0.821
	T2	0.045	–	0.000	0.000	0.021	0.256	0.200	0.012	0.141	0.185	0.176	0.166	0.827
	T3	4.671	6.856	–	0.331	0.093	0.000	0.002	0.041	0.005	0.010	0.008	0.015	0.001
	T4	3.356	4.729	0.982	–	0.143	0.000	0.005	0.159	0.016	0.019	0.017	0.047	0.002
	T5	1.991	2.381	1.712	1.489	–	0.002	0.103	0.855	0.228	0.207	0.251	0.351	0.049
	T6	0.909	1.149	3.947	4.284	3.190	–	0.633	0.067	0.472	0.506	0.582	0.586	0.429
	T7	1.107	1.298	3.325	2.965	1.661	0.480	–	0.078	0.711	0.760	0.804	0.758	0.255
	T8	2.302	2.621	2.097	1.430	0.184	1.873	1.798	–	0.100	0.195	0.206	0.329	0.013
	T9	1.264	1.496	2.939	2.496	1.221	0.724	0.373	1.675	–	0.904	0.908	0.985	0.088
	T10	1.254	1.344	2.663	2.430	1.279	0.670	0.307	1.313	0.122	–	0.982	0.930	0.113
	T11	1.235	1.373	2.742	2.459	1.161	0.555	0.249	1.282	0.116	0.023	–	0.877	0.079
	T12	1.271	1.404	2.529	2.038	0.941	0.548	0.310	0.986	0.019	0.089	0.156	–	0.025
	T13	0.228	0.219	3.662	3.306	2.015	0.797	1.152	2.563	1.739	1.615	1.791	2.304	–

REFERENCES

[1] SAE International, "SAE Levels of Driving Automation™ Refined for Clarity and International Audience," 3 May 2021.

[2] P. Koopman and M. Wagner, "Autonomous vehicle safety: an interdisciplinary challenge," IEEE Intell. Transp. Syst. Mag. **9**, 90–96 (2017).

[3] A. Rolnick and R. E. Lubow, "Why is the driver rarely motion sick? The role of controllability in motion sickness," Ergon. **34**, 867–879 (1991).

[4] C. Diels and J. E. Bos, "Self-driving carsickness," Appl. Ergon. **53**, 374–382 (2016).

[5] C. Jicol, C. H. Wan, B. Doling, C. H. Illingworth, J. Yoon, C. Headey, C. Lutteroth, M. J. Proulx, K. Petrini, and E. O. Neill, "Effects of emotion and agency on presence in virtual reality," *Conf. on Human Factors in Computing Systems - Proc.* (ACM, New York City, NY, 2021), pp. 1–13.

[6] S. Weech, S. Kenny, and M. Barnett-Cowan, "Presence and cybersickness in virtual reality are negatively related: A review," Frontiers in Psychology **10**, 158 (2019).

[7] M. E. McCauley and T. J. Sharkey, "Cybersickness: Perception of self-motion in virtual environments," Presence: Teleoperators and Virtual Environments **1**, 311–318 (1992).

[8] L. J. Jr., "A discussion of cybersickness in virtual environments," ACM SIGCHI Bull. **32**, 47–56 (2000).

[9] J. T. Reason and J. J. Brand, *Motion Sickness* (Academic Press, New York, 1975).

[10] A. K. T. Ng, L. K. Y. Chan, and H. Y. K. Lau, "A study of cybersickness and sensory conflict theory using a motion-coupled virtual reality system," Displays **61**, 101922 (2020).

[11] S. Ishak, A. Bubka, and F. Bonato, "Visual occlusion decreases motion sickness in a flight simulator," Perception **47**, 521–530 (2018).

[12] M. McGill, A. Ng, and S. Brewster, "I am the passenger: How visual motion cues can influence sickness for in-car VR," *Conf. on Human Factors in Computing Systems - Proc.* (ACM, New York City, NY, 2017), pp. 5655–5668.

[13] Y. Y. Kim, H. J. Kim, E. N. Kim, H. D. Ko, and H. T. Kim, "Characteristic changes in the physiological components of cybersickness," Psychophysiology **42**, 616–625 (2005).

[14] B. C. Min, S. C. Chung, Y. K. Min, and K. Sakamoto, "Psychophysiological evaluation of simulator sickness evoked by a graphic simulator," Appl. Ergon. **35**, 549–556 (2004).

[15] R. Liu, E. Peli, and A. D. Hwang, "Measuring visually induced motion sickness using wearable devices," *Proc. IS&T Electronic Imaging: Human Vision and Electronic Imaging* (IS&T, Springfield, VA, 2017), pp. 218–223.

[16] X. Li, C. Zhu, C. Xu, J. Zhu, Y. Li, and S. Wu, "VR motion sickness recognition by using EEG rhythm energy ratio based on wavelet packet transform," Comput. Methods Programs Biomed. **188**, 105266 (2020).

[17] Y. Li, A. Liu, and L. Ding, "Machine learning assessment of visually induced motion sickness levels based on multiple biosignals," Biomed. Signal Process. Control **49**, 202–211 (2019).

[18] M. Recenti, C. Ricciardi, R. Aubonnet, I. Picone, D. Jacob, H. Á. R. Svansson, S. Agnarsdóttir, G. H. Karlsson, V. Baeringsdóttir, H. Petersen, and P. Gargiulo, "Toward predicting motion sickness using virtual reality and a moving platform assessing brain, muscles, and heart signals," Frontiers in Bioengineering and Biotechnology **9**, 132 (2021).

[19] P. Vepakomma, D. De, S. K. Das, and S. Bhansali, "A-Wristocracy: Deep learning on wrist-worn sensing for recognition of user complex activities," *2015 IEEE 12th Int'l. Conf. on Wearable and Implantable Body Sensor Networks, BSN* (IEEE, Piscataway, NJ, 2015).

[20] C. A. Ronao and S. B. Cho, "Human activity recognition with smartphone sensors using deep learning neural networks," Expert Syst. Appl. **59**, 235–244 (2016).

[21] Y. Banchi, K. Tsuchiya, M. Hirose, R. Takahashi, R. Yamashita, and T. Kawai, "Evaluation and estimation of discomfort during continuous work with mixed reality systems by deep learning," *Proc. IS&T Electronic Imaging: Stereoscopic Displays and Applications* (IS&T, Springfield, VA, 2022), pp. 309-1–309-4.

[22] J. Häkkinen, F. Ohta, and T. Kawai, "Time course of sickness symptoms with HMD viewing of 360-degree videos," J. Imaging Sci. Technol. 60403-1–60403-11 (2018).

[23] C.-T. Lin, S.-F. Tsai, and L.-W. Ko, "EEG-based learning system for online motion sickness level estimation in a dynamic vehicle environment," IEEE Trans. Neural Netw. Learning Systems **24**, 1689–1700 (2013).

[24] T. M. Lee, J.-C. Yoon, and I.-K. Lee, "Motion sickness prediction in stereoscopic videos using 3D convolutional neural networks," IEEE Trans. Vis. Comput. Graphics **25**, 1919–1927 (2019).

[25] R. S. Kennedy, N. E. Lane, K. S. Berbaum, and M. G. Lilienthal, "Simulator sickness questionnaire: An enhanced method for quantifying simulator sickness," Int. J. Aviation Psychology **3**, 203–220 (1993).

[26] Y. Wang, J.-R. Chardonnet, and F. Merienne, "VR sickness prediction for navigation in immersive virtual environments using a deep long short term memory model," *2019 IEEE Conf. on Virtual Reality and 3D User Interfaces (VR)* (IEEE, Piscataway, NJ, 2019), pp. 1874–1881.